

Methylcyclohexane Dehydrogenation for Hydrogen Production via a Bimodal Catalytic Membrane Reactor

Lie Meng, Xin Yu, Takuya Niimi, Hiroki Nagasawa, Masakoto Kanezashi, Tomohisa Yoshioka, and Toshinori Tsuru

Dept. of Chemical Engineering, Graduate School of Engineering, Hiroshima University, 1-4-1 Kagami-yama, Higashi-Hiroshima 739-8527, Japan

DOI 10.1002/aic.14764

Published online March 2, 2015 in Wiley Online Library (wileyonlinelibrary.com)

The dehydrogenation of methylcyclohexane (MCH) to toluene (TOL) for hydrogen production was theoretically and experimentally investigated in a bimodal catalytic membrane reactor (CMR), that combined Pt/Al₂O₃ catalysts with a hydrogen-selective organosilica membrane prepared via sol-gel processing using bis(triethoxysilyl) ethane (BTESE). Effects of operating conditions on the membrane reactor performance were systematically investigated, and the experimental results were in good agreement with those calculated by a simulation model with a fitted catalyst loading. With H₂ extraction from the reaction stream to the permeate stream, MCH conversion at 250°C was significantly increased beyond the equilibrium conversion of 0.44–0.86. Because of the high H₂ selectivity and permeance of BTESE-derived membranes, a H₂ flow with purity higher than 99.8% was obtained in the permeate stream, and the H₂ recovery ratio reached 0.99 in a pressurized reactor. A system that combined the CMR with a fixed-bed prereactor was proposed for MCH dehydrogenation. © 2015 American Institute of Chemical Engineers AIChE J, 61: 1628–1638, 2015

Keywords: membrane reactor, organosilica membrane, methylcyclohexane dehydrogenation, hydrogen production

Introduction

As a clean energy carrier, hydrogen is considered one of the key alternatives for the replacement of petroleum products, and is expected to play a significant role in the reduction of the emissions of greenhouse gases for a better environment and sustainable development.^{1,2} For the large-scale utilization of hydrogen, many fundamental scientific and technological challenges are yet to be overcome, such as hydrogen storage and transportation due to the extremely low volumetric density of gaseous hydrogen.³ Some studies have revealed that one feasible solution to efficiently store and safely transport hydrogen is to use liquid organic hydrides that possess relatively high gravimetric storage densities as hydrogen carriers.^{4,5} These liquid organic hydrogen carriers, aromatic compounds, are hydrogenated for storage and dehydrogenated again when hydrogen is needed. The simplest example is the cyclohexane (CH)–benzene–hydrogen cycle. That cycle cannot be seriously considered for actual use, however, because benzene is carcinogenic and it has a high freezing point of 5.5°C. The methylcyclohexane (MCH)–toluene (TOL)–hydrogen cycle has shown the most promise of the liquid organic hydride cycles for hydrogen storage because it is extremely reversible, highly selective, and free of carcinogenic products.⁶ MCH contains 47.4 g of H₂ per liter, and the storage density of H₂ is 6.16 wt %. Moreover, the freezing temperatures of MCH and TOL are

–126.6 and –95°C, respectively, which indicates that these will not freeze under operating conditions in plants. In this cycle, gaseous hydrogen is first reacted with TOL to form MCH. Hydrogen is released by the dehydrogenation of MCH, and the produced TOL is recycled. At ambient temperature and pressure, TOL and MCH are in a liquid state, thus hydrogen can be stored and transported in a safe manner using conventional technologies. However, the dehydrogenation reaction of MCH to TOL is strongly limited by thermodynamic equilibrium, and a shift in equilibrium is required to enhance the equilibrium conversion at low temperatures for practical applications.

A catalytic membrane reactor (CMR) is a combination of a permselective membrane and heterogeneous catalysts.^{7,8} CMRs have the inherent capability and advantage of combining reaction and separation in a single unit. The membrane provides selective removal of one of the components in parallel with a reversible reaction, which shifts the equilibrium toward the product side and thus results in a higher reaction conversion even at lower temperatures.^{9–11} Moreover, because of a lower reaction temperature, CMRs may avoid thermal deactivation of catalysts such as sintering. Because equilibrium-limited reactions usually take place at high temperatures, the membranes used for CMRs are mainly metal or ceramic, such as palladium,^{12–14} dense perovskite,^{15–17} zeolite,^{18,19} and porous ceramic membranes.^{20,21} In addition, the available membranes must provide sufficient permeability and/or permselectivity and always provide long-term stability in both mechanical and chemical properties under technical conditions.²² Considerable research effort has been devoted to the utilization of CMRs for

Correspondence concerning this article should be addressed to T. Tsuru at tsuru@hiroshima-u.ac.jp.

Table 1. Hydrogen Production in Membrane Reactors

| Reaction System | | Reaction Temperature (°C) | Catalysts | Dry or Steamed | Permeate/Retentate |
|-----------------------------|---|---------------------------|-----------|----------------|---------------------------------------|
| Steam reforming of methane | $\text{CH}_4 + 2\text{H}_2\text{O} \leftrightarrow \text{CO}_2 + 4\text{H}_2$ $\Delta H = +164.5 \text{ kJ mol}^{-1}$ | 500–600 | Ni | Hydrothermal | $\text{H}_2/\text{CH}_4, \text{CO}_2$ |
| NH_3 decomposition | $\text{NH}_3 \leftrightarrow 0.5\text{N}_2 + 1.5\text{H}_2$ $\Delta H = +46 \text{ kJ mol}^{-1}$ | 400–500 | Ru | Dry | $\text{H}_2/\text{NH}_3, \text{N}_2$ |
| MCH dehydrogenation | $\text{C}_6\text{H}_{11}\text{-CH}_3 \leftrightarrow \text{C}_6\text{H}_5\text{-CH}_3 + 3\text{H}_2$ $\Delta H = +204.6 \text{ kJ mol}^{-1}$ | 200–300 | Pt | Dry | $\text{H}_2/\text{TOL}, \text{MCH}$ |

hydrogen production from hydrogen carriers, including methane steam reforming,^{23–26} NH_3 decomposition,^{27,28} and the dehydrogenation of CH_4 ^{29–31} and MCH.^{32,33} Table 1 summarizes the typical reactions used for hydrogen production in membrane reactors. All of these reactions are endothermic thermodynamically limited systems, meaning that a high-temperature energy supply is needed for complete conversion. Compared with reactions such as the steam reforming of methane (>500°C) and NH_3 decomposition (>400°C) that are conducted at high temperatures, the dehydrogenation of MCH exhibits the advantages of much lower reaction temperatures that reach a maximum of 300°C. Rahimpour and coworkers³⁴ recently developed a thermally coupled double membrane reactor (TCDMR) for simultaneous exothermic reactions (i.e., methanol synthesis) with endothermic reactions (i.e., MCH dehydrogenation) to produce pure H_2 . They predicted the performance of TCDMR with a steady-state heterogeneous model and demonstrated the superiority of this innovative configuration to the conventional reactors. Ali et al.³⁵ experimentally investigated the MCH dehydrogenation reaction in a CMR using a tubular Pd-Ag membrane, and the yields of TOL and hydrogen were enhanced due to the selective *in situ* removal of hydrogen. However, the higher temperature increased permeation rate setting up an activated diffusion mechanism where hydrogen permeated the Pd-Ag membrane. Therefore, Pd-Ag membranes may not be suitable for MCH dehydrogenation due to decreased H_2 permeability caused by a low-temperature operation. In addition, a larger difference in molecular size between hydrogen and other components allows porous membranes with a high selectivity for hydrogen over other gases to be alternative materials for hydrogen production. Porous silica membranes fit into this category. Moreover, the dry conditions of MCH dehydrogenation makes the utilization of porous silica membranes much more attractive because silica-based microporous membranes have shown excellent separation performance for hydrogen and high stability in a wide temperature range when used under moisture-free conditions.^{23,28}

Previously, we proposed a novel bimodal CMR that consisted of a separation layer and a bimodal catalytic layer.³⁶ Compared with packed-bed membrane reactors, the bimodal CMR provides the shorter path for conversion and transport due to the closer distance between the catalysts and the membrane, and correspondingly lower resistance. The bimodal CMR has been demonstrated capable of breaking the performance restraints related to mass-transfer limitation, such as H_2 dilution and concentration polarization which occurs on the membrane surface caused by the selective extraction of H_2 .^{36,37} For MCH dehydrogenation in a bimodal CMR, MCH conversion was highly enhanced from 0.49 to 0.71 at 220°C because of the H_2 extraction via the membrane derived from tetraethoxysilane (TEOS).³⁰ Recently, we reported a strategy whereby silica networks were designed using bis(triethoxy-

silyl) ethane (BTESE) as a silica precursor in the development of a highly permeable hydrogen separation membrane,^{38,39} and these membranes have been successfully applied for MCH dehydrogenation in membrane reactors.^{40,41} However, the effects of membrane reactor configuration and operating conditions on the performance of membrane reactors have not been extensively investigated.

In the present study, a bimodal CMR (Figure 1) consisting of a Pt/ γ - Al_2O_3 / α - Al_2O_3 catalytic support and a BTESE-derived silica layer which is a new class of H_2 separation membranes, was prepared and applied to MCH dehydrogenation for hydrogen production, and was studied theoretically and experimentally. A one-dimensional (1-D) isothermal plug-flow model was employed to simulate a cocurrent configuration membrane reactor. The effects of operating conditions (e.g., reaction temperature, MCH feed flow rate, and feed pressure) on membrane reactor performance in terms of MCH conversion, H_2 yield, H_2 purity, total H_2 flow rate, and H_2 recovery ratio were systematically investigated and compared with those predicted by the proposed simulation model. An improved MCH conversion up to 0.99 and a H_2 recovery ratio as high as 0.99 were successfully achieved in the bimodal CMR. Moreover, a system combining a fixed-bed prereactor and a CMR for MCH dehydrogenation was discussed.

Simulation

The mathematical model of MCH dehydrogenation in the bimodal CMR considered the following hypotheses: (1) steady-state operation; (2) plug flow in retentate and permeate streams; (3) isothermal reaction, which only occurs over the catalyst on the retentate side; (4) negligible pressure drop along the axial direction of the membrane reactor; and, (5) no concentration polarization effect for gas permeation through the membrane. A schematic model for the membrane reactor used in the simulations is shown in Figure 2.

The molar flow rates for each species in the retentate and permeate streams are given by Eqs. 1 and 2, respectively^{23,28}:

Feed stream

$$\frac{dF_i}{dz} = r_d w_{\text{cat}} - s P_i (x_i p_R - y_i p_P) \quad (1)$$

Permeate stream

$$\frac{dQ_i}{dz} = s P_i (x_i p_R - y_i p_P) \quad (2)$$

where F_i and Q_i represent the flow rates of the i th component in the feed and permeate streams, and the corresponding mole fractions are denoted as x_i and y_i , respectively; z indicates the axial direction along the membrane; w_{cat} and s are the weight of catalysts and membrane area per membrane unit length, respectively; P_i is the permeance of the i th component through the membrane; and, p_R and p_P indicate the

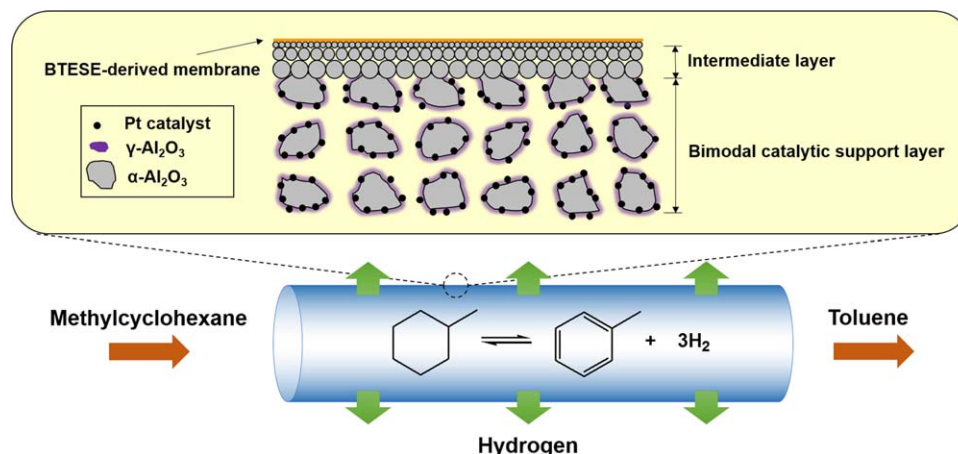


Figure 1. Schematic diagram of the bimodal catalytic membrane reactor.

[Color figure can be viewed in the online issue, which is available at wileyonlinelibrary.com.]

pressure of the feed and permeate streams, respectively. Also, r_d is defined as the reaction rate of MCH dehydrogenation, which can be described as follows^{33,42}

$$r_d = k_1 p_{\text{MCH}} \left(1 - \frac{p_{\text{TOL}} p_{\text{H}_2}^3}{K_{\text{eq}} p_{\text{MCH}}} \right) \quad (3)$$

where K_{eq} is the equilibrium constant for the MCH dehydrogenation and can be calculated by thermodynamic analysis. The reaction rate constant is as follows

$$k_1 = \exp \left(11.4 - \frac{112000}{RT} \right) \quad (4)$$

MCH dehydrogenation over Pt/Al₂O₃ catalyst follows a two-step nonequilibrium mechanism in which MCH is adsorbed and converted to TOL on the surface in the first step and the TOL formed is desorbed from the surface in the following step.⁴³ The simulation of MCH dehydrogenation was conducted in a cocurrent configuration membrane reactor. The reaction temperature, MCH feed flow rate, and feed pressure were adopted as parameters to study their effect on membrane reactor performance in terms of MCH conversion, H₂ yield, H₂ purity, H₂ flow rate, and H₂ recovery ratio. MCH conversion (X) in the membrane reactor is defined as the percentage of reacted MCH, and is expressed in the following equation

$$X = \frac{F_{\text{MCH},0} - F_{\text{MCH},L} - Q_{\text{MCH},L}}{F_{\text{MCH},0}} \quad (5)$$

where $F_{\text{MCH},0}$ refers to the flow rates of MCH entering the membrane reactor in the feed stream.

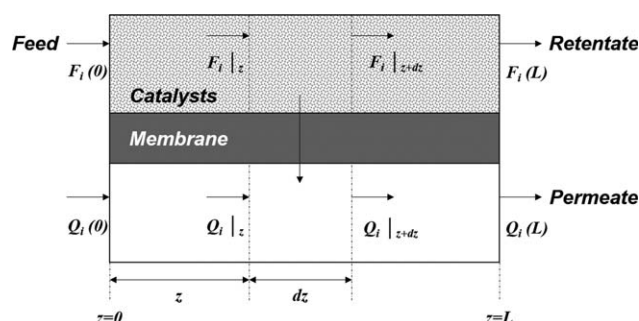


Figure 2. Schematic model for membrane reactor simulation.

H₂ yield (Y) is calculated by dividing the amount of obtained H₂ in the permeate stream by the theoretical yield of H₂, and is described as follows

$$Y = \frac{Q_{\text{H}_2,L}}{3F_{\text{MCH},0}} \quad (6)$$

H₂ recovery ratio (R) is defined as the ratio of the permeate H₂ flow rate to total produced H₂ flow rate, as follows:

$$R = \frac{Q_{\text{H}_2,L}}{F_{\text{H}_2,L} + Q_{\text{H}_2,L}} \quad (7)$$

Without H₂ extraction, H₂ purity (G_{feed}) in the reaction stream is described by the following equation

$$G_{\text{feed}} = \frac{F_{\text{H}_2,L}}{F_{\text{MCH},L} + F_{\text{TOL},L} + F_{\text{H}_2,L}} \quad (8)$$

With H₂ extraction, H₂ purity (G_{permeate}) is calculated as the ratio of the permeate H₂ flow rate to the total flow rate in permeate stream, as follows

$$G_{\text{permeate}} = \frac{Q_{\text{H}_2,L}}{Q_{\text{MCH},L} + Q_{\text{TOL},L} + Q_{\text{H}_2,L}} \quad (9)$$

Experimental

Preparation and characterization of bimodal catalytic membranes

Tubular, porous α -alumina substrates with a porosity of 50%, an active length of approximately 100 mm, an outer diameter of 10 mm, and an average pore diameter of 1 μm were used as the supports for BTESE-derived silica membranes. The first step was to prepare a Pt/ γ -Al₂O₃/ α -Al₂O₃ catalytic support. In order to increase the surface area for catalyst impregnation, a boehmite sol (Nissan Chemical Industries, Japan) was impregnated into the macropores of the α -Al₂O₃ tube to fabricate a γ -/ α -Al₂O₃ bimodal support, which was followed by firing at 550°C. The support was then immersed in a H₂PtCl₆ (Sigma-Aldrich, Japan) solution (25 wt %) and calcined at 500°C for 3 h to form a Pt/ γ -Al₂O₃/ α -Al₂O₃ catalytic support with a Pt loading of 0.11 g (1.0 wt %). The second step was to sequentially coat α -Al₂O₃ particles, SiO₂-ZrO₂ sol, and BTESE-derived silica sol onto the as-prepared catalytic support. The details of this preparation procedure were described earlier.^{36,40,41}

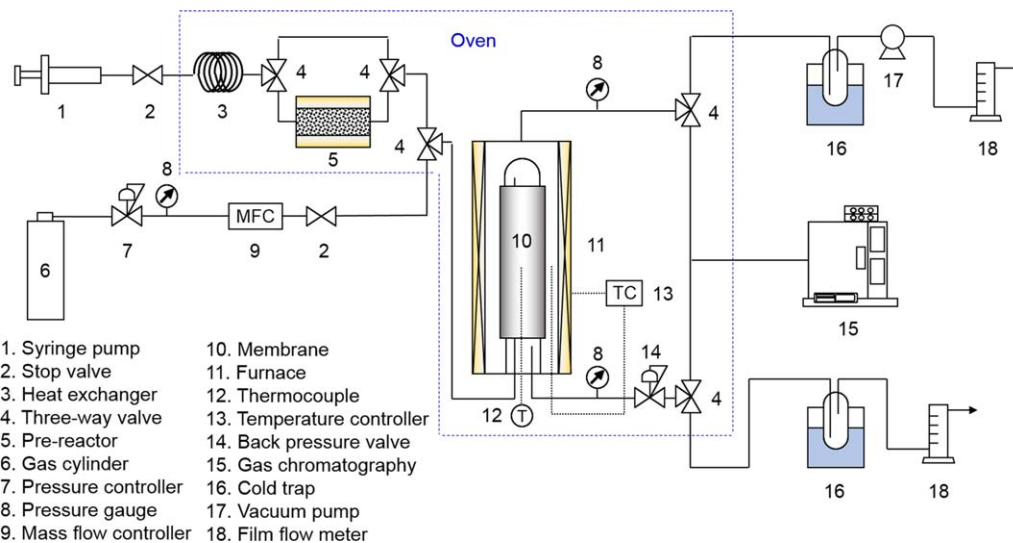


Figure 3. Experimental apparatus for single-gas permeation tests and MCH dehydrogenation.

[Color figure can be viewed in the online issue, which is available at wileyonlinelibrary.com.]

The morphology of the BTESE-derived silica membrane was examined by scanning electron microscopy (SEM) (JCM-5700, JEOL, Japan). The gas permeation properties of the membrane were evaluated by single-gas permeation tests at 200°C using He, H₂, N₂, CH₄, C₃H₈, and TOL, with a transmembrane pressure of 0.1–0.2 MPa. The gas flow rate through the membrane was measured using a film flow meter (SF-2U, Horiba, Japan).

MCH dehydrogenation in the bimodal CMR

Figure 3 shows the experimental apparatus for MCH dehydrogenation in a bimodal CMR. MCH was fed inside the membrane by a syringe pump at a flow rate that ranged from 1.1×10^{-6} to 20.0×10^{-6} mol s⁻¹. Then, the MCH was allowed to evaporate in a wired heat-exchanger in an oven controlled at 110°C. The feed side was controlled with a back-pressure regulator and pressurized from 0.10 to 0.23 MPa, while the permeate stream was kept at a pressure of 10 kPa using a vacuum pump (DAP-6D, ULVAC KIKO, Japan). The temperature inside the membrane was varied between 230 and 270°C, and the membrane module was set in an oven controlled at 110°C to avoid any possible condensation. The compositions and flow rates of both permeate and retentate were determined by means of a gas chromatograph (GC-14B, Shimadzu, Japan) equipped with a thermal conductivity detector and a BX-10 column using Ar as the carrier gas and film flow meters set after the cold traps, respectively. To further improve the membrane reactor performance for MCH dehydrogenation, a packed-bed prereactor was introduced before the membrane reactor. Pt/ γ -Al₂O₃ (2.0 wt %) catalyst (1.1 g) prepared by incipient wetness impregnation was packed into the prereactor, and the temperature of the prereactor was kept at 250°C.

Results and Discussion

Characterization of bimodal catalytic membranes

Figure 4 shows the SEM image of the cross-section of a BTESE-derived silica membrane, in which the Pt/ γ -Al₂O₃/ α -Al₂O₃ catalytic support layer, α -Al₂O₃ and SiO₂-ZrO₂ intermediate layer, and BTESE-derived silica layer were all clearly identifiable. The BTESE-derived silica layer fabri-

cated from a sol-gel process for H₂ separation was continuous and crack-free, and it was less than 200 nm in thickness.

For MCH dehydrogenation in a CMR, the molecular sieving characteristics of the membranes are key criteria. Given the components involved in this system, H₂ (kinetic diameter = 0.29 nm), TOL (kinetic diameter = 0.59 nm), and MCH (kinetic diameter = 0.60 nm),⁴⁴ a membrane pore size controlled in a narrow distribution was expected to enhance the H₂ separation efficiency and achieve a high H₂ purity. The quality of the bimodal catalytic membranes was characterized by the single-gas permeances, which were given as a function of the kinetic diameter of the gas molecules. Figure 5 shows the kinetic diameter dependence of gas permeances for the BTESE-derived membrane and the previously reported TEOS-derived membrane,³⁶ which corresponds to the pore-size distribution of these porous membranes. The single-gas permeances at 200°C generally decreased with increases in kinetic diameter. The BTESE-derived organosilica membrane showed ~ 1 order of magnitude higher H₂ permeance ($\sim 10^{-6}$ mol m⁻² s⁻¹ Pa⁻¹) than the TEOS-derived silica membrane, and the selectivities of H₂/C₃H₈ and H₂/TOL were 55,000 and 16,000, respectively. The H₂/TOL

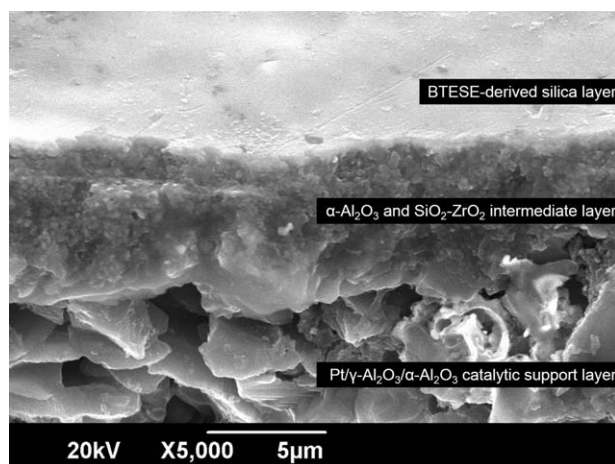


Figure 4. SEM image of the cross-section of a BTESE-derived silica membrane.

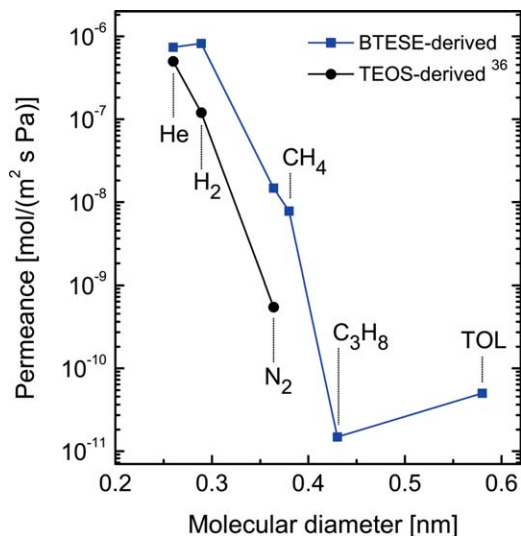


Figure 5. Kinetic diameter dependence of gas permeances for a BTESE-derived organosilica membrane and for previously reported TEOS-derived silica membranes³⁶ at 200°C.

[Color figure can be viewed in the online issue, which is available at wileyonlinelibrary.com.]

selectivity of 16,000 was much higher than the Knudsen selectivity of 6.8, which indicated that H₂ could be effectively extracted from MCH-TOL-H₂ mixtures. Conversely, the membrane used in this work exhibited a relatively lower H₂/N₂ selectivity, which could be attributed to the much looser structure of BTESE, as reported in our previous study.³⁸ With a modified gas transport model,⁴⁵ we proposed to quantitatively calculate the pore-size distribution, the mean pore size of BTESE-derived membranes used in this work was found to be 0.44 nm.

The separation performances of several inorganic membranes used for the dehydrogenation of TOL or CH in membrane reactors is summarized in Table 2. Among those inorganic membranes from the published literature, the BTESE-derived membrane studied in this work shows the most impressive gas transport properties. In particular, the H₂ selectivity was much higher than that of Vycor glass,³² alumina,⁴⁶ FAU zeolite,²⁹ or tetramethoxysilane,³⁰ yet it was approximately the same, or even higher, than that of dimethoxydiphenylsilane (DMDPS), which was obtained using chemical vapor deposition (CVD).³⁰ BTESE-derived membranes prepared via the sol-gel method also exhibited a H₂ permeance that was higher than 10⁻⁶ mol m⁻² s⁻¹ Pa⁻¹ while maintaining a high H₂/TOL selectivity, which confirmed that better pore size control in a silica network for H₂ separation could be achieved using BTESE as a silica precursor and the sol-gel method for membrane preparation. In addition, Figure 6 graphically compares the results from this work with those previously reported and shows how the BTESE-derived membrane surpassed an upper-bound line drawn through the performance of those various inorganic membranes. The highlighted BTESE exhibited an extraordinary combination of selectivity and permeance for H₂. Furthermore, the comparison between the BTESE-derived membrane used in this work and those reported in our previous study⁴¹ shows that the performances of BTESE-derived membranes prepared by sol-gel processing are reproducible. These results demonstrate that the BTESE-derived membrane

is an attractive alternative material for high-purity production in a MCH-TOL-H₂ cycle.

Time course of MCH dehydrogenation in CMRs

Figure 7 shows the time course for MCH conversion, H₂ flow rate, and H₂ purity in the BTESE-derived CMR at 270°C under a reaction pressure that was fixed at 0.1 MPa. In the first stage (reaction time: 0–50 min), the membrane reactor was operated without hydrogen extraction. The MCH conversion was approximately 0.60, which is lower than the thermodynamic equilibrium of 0.74. The reason might be that the residence time was insufficient to reach the equilibrium conversions. However, a steady H₂ flow of 7.9×10^{-6} mol s⁻¹ was obtained in the feed stream, indicating the MCH decomposition on the reaction side was maintained in a stable manner. After 60 min of reaction time, H₂ was extracted from the reaction stream to the permeate stream by evacuating at 10 kPa using a vacuum pump. Due to the shift in the reaction equilibrium, MCH conversion was significantly increased from 0.60 to 0.97 despite the insufficient residence time, and the total H₂ flow rate. The sum of the H₂ flow rates of both reaction and permeate stream, was raised to 11.4×10^{-6} mol s⁻¹. A steady H₂ flow of 11.0×10^{-6} mol s⁻¹ was obtained in the permeate stream, while a much smaller H₂ flow of 0.4×10^{-6} mol s⁻¹ was detected in the retentate stream. The corresponding H₂ recovery ratio was 0.96, indicating that most of the H₂ generated in the retentate stream permeated to the permeate side. In the permeate stream, H₂ purity was higher than 99.7% while a small amount of MCH and TOL was detected, confirming that the BTESE-derived membrane was virtually impermeable to MCH and TOL.^{40,41} At 170 min when the H₂ extraction was stopped, the MCH conversion, H₂ flow rate and H₂ purity decreased to the values that were almost the same as that before H₂ extraction, confirming the good stability of the membrane reactor. It should be noted that the mass balances for C and H atoms between the inlet and the outlet of the reactor were kept lower than 10%.

Effect of operation conditions on membrane reactor performance

Figure 8 shows the MCH conversion, H₂ yield, H₂ purity, total H₂ flow rate, and H₂ recovery ratio as a function of the reaction temperature with/without H₂ extraction. The feed flow rate of MCH was kept at 4×10^{-6} mol s⁻¹. The reaction temperature played an important role in the performance of the membrane reactor via thermodynamics and kinetics.⁴⁷ As shown, the MCH conversion with/without H₂ extraction obviously was increased with increases in the reaction temperature regardless of the extraction of the produced hydrogen, because MCH dehydrogenation is an endothermic reaction. When the reactor was operated without H₂ extraction with an increase in temperature from 230 to 270°C, the MCH conversion could not exceed the equilibrium conversion, and the total H₂ flow rate varied at between 3.0 and 8.0×10^{-6} mol s⁻¹ with a H₂ purity lower than 70.0%. For the bimodal CMR with the BTESE-derived membrane, there was a significant increase in MCH conversion due to the selective extraction of produced H₂ from the reaction stream to the permeate stream, leading to a shift in the thermodynamic equilibrium and an enhancement in conversion. As a result, the total H₂ flow rate markedly increased and the H₂ purity in the permeate stream was always higher than 99.8%.

Table 2. Comparison of the Separation Performance of Inorganic Membranes Used for the Dehydrogenation of Methylcyclohexane or Cyclohexane

| Membranes | H ₂ Permeance (10 ⁻⁷ mol/[m ² s Pa]) | H ₂ /Toluene or H ₂ /Cyclohexane | Temperature (°C) | Preparation Methods | References |
|---------------------------------|---|--|------------------|---------------------|------------|
| Alumina | 32.2 | 7.0 | 200 | Sol-gel | 46 |
| Vycor glass | 0.3 | 7.9 | 250 | — | 32 |
| FAU zeolite | 7.1 | 14.2 | 200 | Hydrothermal | 29 |
| Tetramethoxysilane (TMOS) | 0.4 | 715 | 200 | CVD | 30 |
| Dimethoxydiphenylsilane (DMDPS) | 9.3 | 3100 | 200 | CVD | 30 |
| BTESE | 8.2 | 16000 | 200 | Sol-gel | This work |

These results reveal that the temperature supplied to the decomposition reaction for obtaining a certain MCH conversion could be decreased via H₂ extraction based on membranes with high H₂ selectivity. Hence, the bimodal CMR significantly increased MCH conversion while simultaneously reducing the reaction temperature. Meanwhile, there was a clear trend of increases in the H₂ yield and recovery ratio when the reaction temperature was elevated, because MCH conversion was enhanced and a higher partial pressure of H₂ was obtained. The H₂ recovery ratio, defined as the ratio of the permeate H₂ flow rate to the total H₂ flow rate produced, showed values higher than 0.94 due to the high H₂ permeance of the BTESE-derived membrane.

To gain further understanding into the effect of reaction temperature in the present system, the bimodal CMR was studied theoretically using simulations under various reaction temperatures. In our modeling, the permeation of H₂ was kept at 10⁻⁶ mol m⁻² s⁻¹ Pa⁻¹, and the selectivities of H₂/MCH and H₂/TOL were both set to 16,000. The values of the membrane area and the feed flow rate of MCH were assumed to be the same as the experimental conditions. Therefore, the weight of the catalysts, w_{cat} , was used as the single fitting parameter in the simulations. As shown in Figure 8, with a fitted value of 2×10^{-3} kg m⁻¹ for w_{cat} (experimental catalyst loading $w_{\text{cat}} = 1.3 \times 10^{-3}$ kg m⁻¹), the simulation results obtained from the membrane reactor

with/without H₂ extraction at different temperatures were in good agreement with the experimental investigation, which verified that our proposed model was effective in predicting the performance of the bimodal CMR. The above results suggested that adjusting the mathematical model by the catalyst loading is a simple but effective simulation strategy for membrane reactors. Nevertheless, one reason for the high accuracy of the simulation in this work might have been that the phenomenon of concentration polarization that frequently occurs along a membrane surface in packed bed membrane reactors was inhibited due to the closer distance between the catalysts and the membrane in the bimodal CMR. That could have had a seriously adverse effect on the performance of the membrane separation.

The relationship between the MCH feed flow rate and the performance of the bimodal CMR is shown in Figure 9. When the permeate stream was kept at atmospheric pressure and at a temperature of 250°C where there was no H₂ extraction, the MCH conversion was approximately equal to the equilibrium conversion of 0.44, but gradually decreased because of a shorter residence time as the MCH feed flow rate increased. When the permeate stream was evacuated to 10 kPa, H₂ permeated through the BTESE-derived membrane, resulting in an enhancement in the MCH conversion and in the total H₂ flow rate. For instance, in the case of a MCH feed flow rate of 1.1×10^{-6} mol s⁻¹, the H₂ extraction increased MCH conversion to 0.99, which was far beyond the equilibrium conversion of 0.47. For MCH decomposition with/without H₂ extraction, the reaction conversion decreased with an increase in the MCH feed flow rate, which could be attributed to the increased space velocity.²⁸ Similar tendencies were observed in both the H₂ yield and H₂ recovery ratio when the MCH feed flow rate was raised, which could be explained by the limited H₂ permeate flux that was restricted by the membrane characteristics such as H₂ permeability and membrane area, as well as by the operational conditions. Therefore, the enhancement of MCH conversion that was assisted by H₂ extraction was lessened, and the MCH conversion approached that without H₂ extraction. Additionally, the H₂ purity in the permeate stream reached 99.8% at an elevated MCH feed flow rate, suggesting that the BTESE-derived membrane was almost impermeable for MCH and TOL. All the curves in Figure 9 showing MCH conversion, H₂ yield, H₂ purity, total H₂ flow rate, and H₂ recovery ratio were simulated using the experimentally obtained permeances of H₂, MCH, and TOL with a fitted value for the catalyst loading under the assumption of an infinite reaction rate. This simulation also agreed with the experimental data, which confirmed the applicability of the present simulation model.

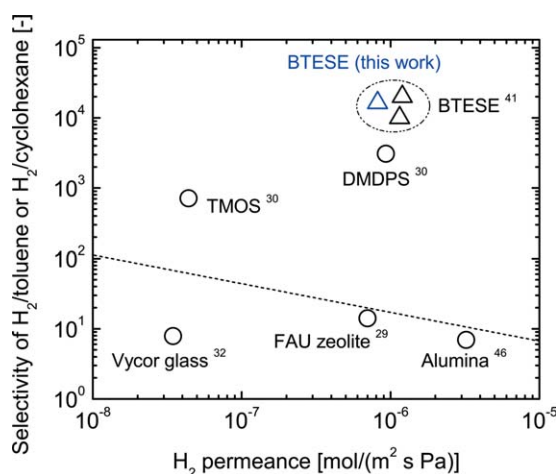


Figure 6. Comparison of the separation performance of inorganic membranes used for the dehydrogenation of MCH or CH in membrane reactors.

[Color figure can be viewed in the online issue, which is available at www.interscience.wiley.com.]

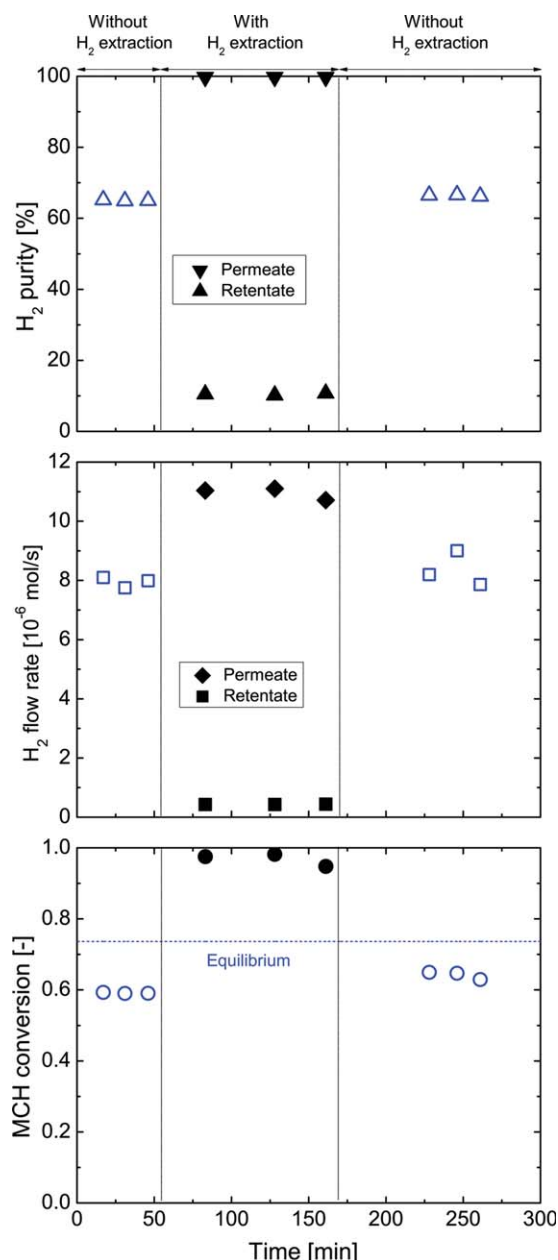


Figure 7. Time course of MCH conversion, H₂ flow rate and H₂ purity with/without H₂ extraction in a bimodal CMR ($T_r = 270^\circ\text{C}$, $p_R = 101.3\text{ kPa}$, $p_P = 10\text{ kPa}$, $F_{\text{MCH},0} = 4 \times 10^{-6}\text{ mol s}^{-1}$).

[Color figure can be viewed in the online issue, which is available at wileyonlinelibrary.com.]

Figure 10 shows the performance of the bimodal CMR at feed pressures that ranged from 0.10 to 0.23 MPa while the pressure in the permeate stream was fixed at 10 kPa. The feed flow rate of the MCH and the reaction temperature were kept at $4 \times 10^{-6}\text{ mol s}^{-1}$ and 250°C , respectively. In the case of the MCH decomposition without H₂ extraction, the MCH conversion was decreased when the reaction pressure was increased, which could be explained using thermodynamics (more moles of products than reactants). Therefore, MCH decomposition operated in a traditional pressurized reactor is unfavorable, although a high-pressure operation is helpful in reducing the reactor size. For a membrane reactor, however, the increased pressure in the feed

stream results in an enhanced driving force for H₂ permeation from the reaction stream to the permeate stream, which may lead to an equilibrium shift that will improve MCH conversion. As shown in Figure 10, with increased feed pressure, the MCH conversion with H₂ extraction was kept at values higher than 0.80, while the MCH conversion without H₂ extraction was decreased to 0.20. When H₂ extraction was employed, as the feed pressure increased from 0.10 to 0.23 MPa, the H₂ yield obviously raised to 0.95, and the total H₂ flow rate reached $10.5 \times 10^{-6}\text{ mol s}^{-1}$ with a H₂ recovery ratio as high as 0.99, which indicated that the H₂ extraction was enhanced due to the increased driving force for H₂ permeation through the membrane. It is noteworthy to mention that the high H₂ recovery ratio, that is 99% of

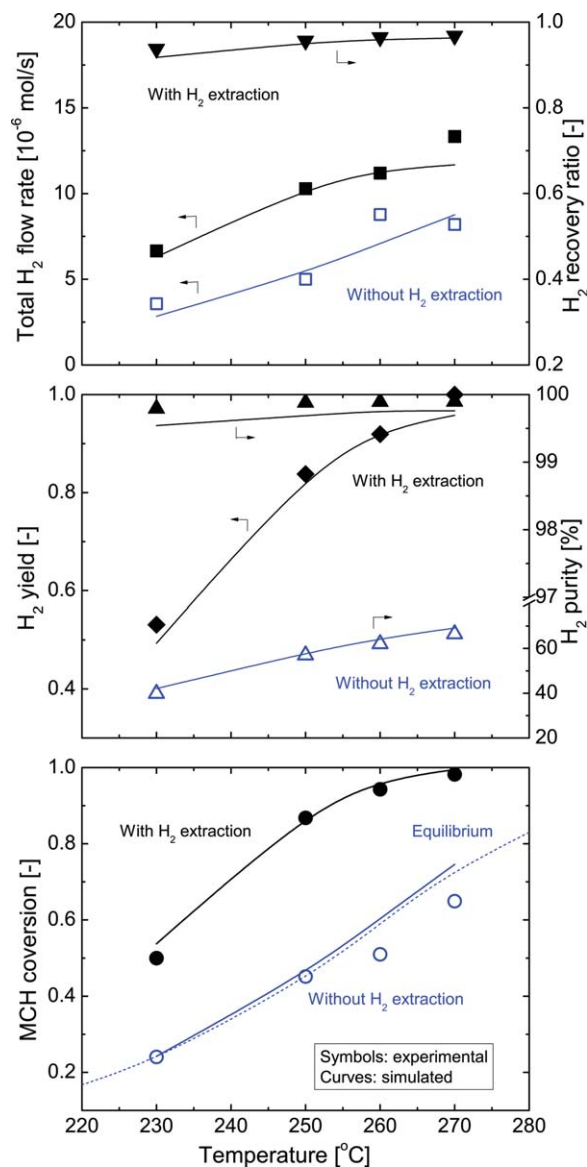


Figure 8. Effect of the reaction temperature on the performance of a bimodal CMR for MCH decomposition with/without H₂ extraction ($p_R = 101.3\text{ kPa}$, $p_P = 10\text{ kPa}$, $F_{\text{MCH},0} = 4 \times 10^{-6}\text{ mol s}^{-1}$).

The curves were simulated with a fitted w_{cat} of $2 \times 10^{-3}\text{ kg m}^{-1}$ with/without H₂ extraction at different temperatures. [Color figure can be viewed in the online issue, which is available at wileyonlinelibrary.com.]

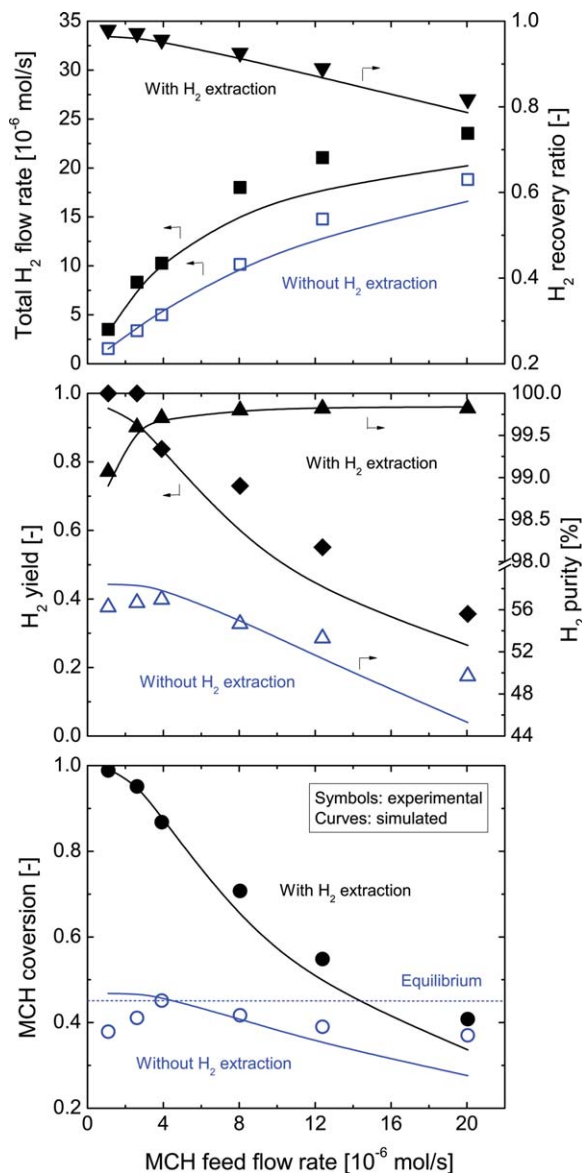


Figure 9. Effect of the MCH feed flow rate on the performance of a bimodal CMR for MCH decomposition with/without H_2 extraction ($T_r = 250^\circ\text{C}$, $p_R = 101.3\text{ kPa}$, $p_P = 10\text{ kPa}$).

Curves were simulated with a fitted w_{cat} of $2 \times 10^{-3}\text{ kg m}^{-1}$ with/without H_2 extraction at different MCH feed flow rates. [Color figure can be viewed in the online issue, which is available at wileyonlinelibrary.com.]

hydrogen produced by the feed MCH recovered at permeate side, could significantly improve the efficiency of H_2 production system and lower the total energy consumption. In addition, the H_2 purity in the permeate stream was higher than 99.4%, confirming the high selectivities of BTESE-derived organosilica membrane for H_2/MCH and H_2/TOL . As the simulation analysis suggested, for a bimodal CMR with appropriate catalytic activity, using a pressurized system to increase the hydrogen partial pressure difference between the retentate and the permeate sides for hydrogen permeation is an effective way to improve the H_2 yield and recovery ratio. It is noteworthy that with only one fitting parameter, catalyst loading, our proposed model was capable of quantitatively simulating the dependency of MCH conversion, H_2 purity, H_2 yield, and H_2 recovery ratio on reaction temperature,

feed flow rate, and feed pressure, as shown in Figures 7, 8, and 9, respectively. There was a slight difference between our experimental and predicted MCH conversions under elevated feed pressure, which was also observed by Akamatsu et al.^{31,33} Their difference was considered to be a result of the decrease in hydrogen permeance caused by the adsorption of MCH and/or TOL in the membrane pores, which could possibly be avoided by tuning the membrane pore sizes and/or by operation at higher temperatures.³⁰ Thus, the bimodal CMR proposed in this work has great potential to improve MCH conversion as well as the H_2 recovery ratio,

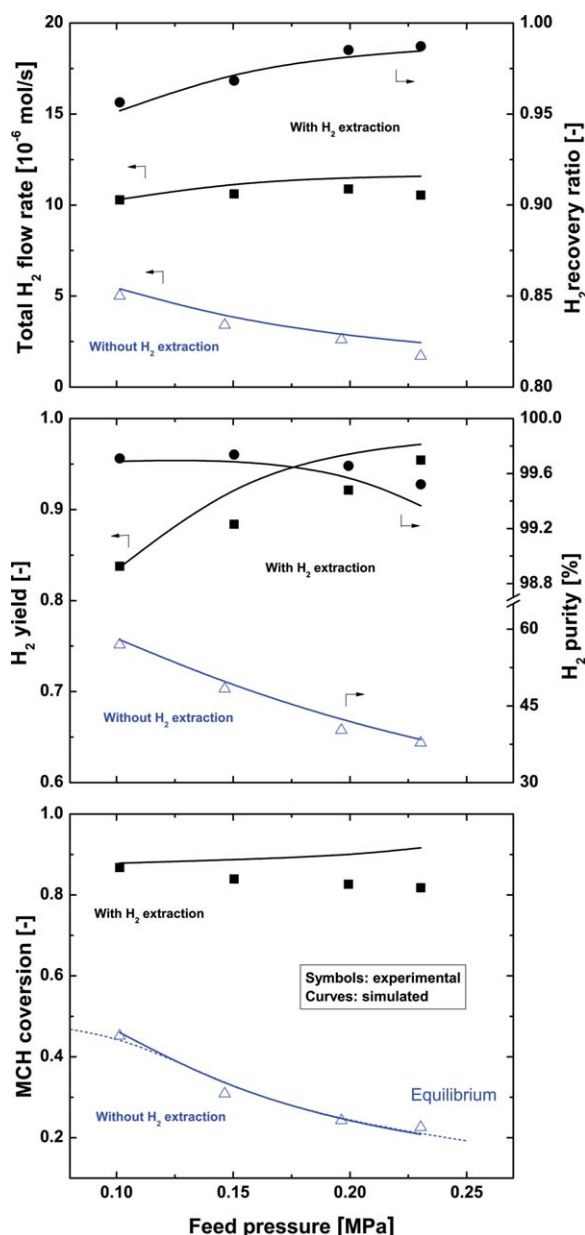


Figure 10. Effect of feed pressure on the performance of a bimodal CMR for MCH decomposition with/without H_2 extraction ($T_r = 250^\circ\text{C}$, $p_P = 10\text{ kPa}$, $F_{\text{MCH},0} = 4 \times 10^{-6}\text{ mol s}^{-1}$).

Curves were simulated with a fitted w_{cat} of $2 \times 10^{-3}\text{ kg m}^{-1}$ with/without H_2 extraction under different feed pressures. [Color figure can be viewed in the online issue, which is available at wileyonlinelibrary.com.]

Table 3. Comparison of the Performance of Catalytic Membrane Reactors used for the Dehydrogenation of Methylcyclohexane

| Membrane | | | Pressure | | $F_{\text{MCH},0}$ (10^{-7} mol s $^{-1}$) | Catalyst | GHSV (h $^{-1}$) | J_{H_2} (mol m $^{-2}$ s $^{-1}$) | X_{MCH} | Reference |
|-------------|------------------|----------------|----------|---------------------------|---|---|----------------------|--|------------------|-----------|
| Material | Diameter (mm) | Length (mm) | T (°C) | (kPa) (Feed/ Permeate) | | | | | | |
| Pd-Ag | 3.1 | 230 | 320 | 1500/100 | 3.1 | Pt/Al $_2$ O $_3$ | 1.0 | 0.28 | 0.51 | 42 |
| Vycor glass | 5.1 | 100 | 180 | 100/100 (sweep) | 5.6 | Pt/Al $_2$ O $_3$, $w_{\text{Pt}} = 0.01$ g | 22.7 | 0.51 | 0.61 | 32 |
| DMDPS | 6.3 | 50 | 220 | 100/100 (sweep) | 13.1 | Pt/Al $_2$ O $_3$ | 67.9 | 1.31 | 0.52 | 33 |
| DMDPS | 6.3 | 50 | 260 | 100/100 (sweep) | 13.1 | Pt/Al $_2$ O $_3$ | 67.9 | 2.40 | 0.95 | 33 |
| BTESE | 10.0 | 84 | 250 | 101/10 | 80.0 | Pt/Al $_2$ O $_3$, $w_{\text{Pt}} = 0.11$ g | 97.9 | 2.62 | 0.72 | This work |
| BTESE | 10.0 | 84 | 270 | 101/10 | 40.0 | Pt/Al $_2$ O $_3$, $w_{\text{Pt}} = 0.11$ g | 48.9 | 1.78 | 0.98 | This work |

and produce high-purity H₂ in a pressurized system of MCH decomposition.

To better evaluate the practical significance of these results, a comparison of the performance of CMRs used for MCH dehydrogenation is necessary. Operation conditions such as reaction temperature (T), pressure (p_R/p_P), MCH feed flow rate ($F_{\text{MCH},0}$, mol s $^{-1}$) as well as gas hourly space velocity (GHSV, h $^{-1}$), and experimental results like MCH conversion (X_{MCH}) and H₂ production rate per unit reactor volume (J_{H_2} , mol m $^{-2}$ s $^{-1}$) obtained from this work and literature are listed in Table 3. The volume of membranes was used as reactor volume in calculation of GHSV and J_{H_2} as the catalysts were often loaded into bore side of tubular membranes in packed-type membrane reactors. So far, silica membranes showed higher MCH conversion and H₂ production rate than other membrane materials even at an increased GHSV, which could be attributed to their excellent permeability and selectivity for H₂.

It is noteworthy that during the investigation of the effect of various operation conditions on the membrane reactor performance, MCH dehydrogenation was carried out in the bimodal CMR for more than 150 h. No significant changes could be observed in catalytic activity and membrane permeability of the membrane reactor, which demonstrated the high stability of the BTESE-derived membrane and Pt catalysts evaluated in this work.

Effect of prereactor on membrane reactor performance

In our previous study, the application of a prereactor before the membrane reactor was an effective method to increase H₂ partial pressure in the feed to the membrane, which successfully improved the performance of a bimodal CMR.³⁷ Thus, the time course of MCH conversion in a bimodal CMR with/without a prereactor was investigated, keeping the temperature inside the membrane at 250°C, as shown in Figure 11. Without H₂ extraction and the assistance of the prereactor, a MCH conversion of approximately 0.44, which was equal to equilibrium conversion, was observed in the membrane reactor during the initial course of the reaction. As the H₂ extraction was carried out, the MCH conversion was increased to 0.86 without the use of a prereactor, due to the equilibrium shift. When a prereactor was used, the MCH conversion, which was defined based on the MCH flow rate entering prereactor, at the outlet of the bimodal CMR was enhanced significantly and reached 0.99. One explanation for the significant effect of the prereactor on reaction conversion could have been that with the prereactor, the MCH decomposition reached equilibrium conversion

before the reaction mixture was fed into the reaction stream of the membrane reactor, which produced a higher H₂ partial pressure at the inlet of the membrane reactor, and therefore, resulted in an increased H₂ permeation rate through the BTESE-derived membrane.³⁷ The other reason might have been that without the use of a prereactor, the MCH decomposition took place in the pores of the catalytic support and thus lowered the temperature inside the membrane as the reaction was endothermic. According to our previous reports, for the BTESE-derived membrane, H₂ permeance was decreased and TOL permeance was increased when permeation temperature was decreased, which lowered the permeation rate as well as the membrane selectivity.⁴¹ Therefore, the temperature distribution in the membrane reactor is an important issue for MCH decomposition.

Figure 12 shows the temperature profile along the axial direction for the bimodal CMR with/without the use of a prereactor. The temperature between the outside of the membrane module and the furnace was controlled at 250°C at the center of the axial direction, and the temperature inside the CMR was measured by moving another thermocouple inside the membrane. The temperature along the axial direction of the membrane gradually decreased from 252 to 243°C under

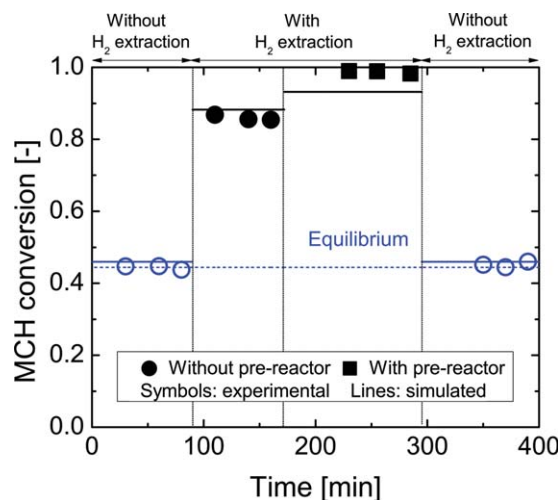


Figure 11. Time course of MCH conversion in the bimodal CMR with/without a prereactor ($T_r = 250^\circ\text{C}$, $p_R = 101.3$ kPa, $p_P = 10$ kPa, $F_{\text{MCH},0} = 4 \times 10^{-6}$ mol s $^{-1}$).

Lines were simulated with a fitted w_{cat} of 2×10^{-3} kg m $^{-1}$. [Color figure can be viewed in the online issue, which is available at www.interscience.wiley.com.]

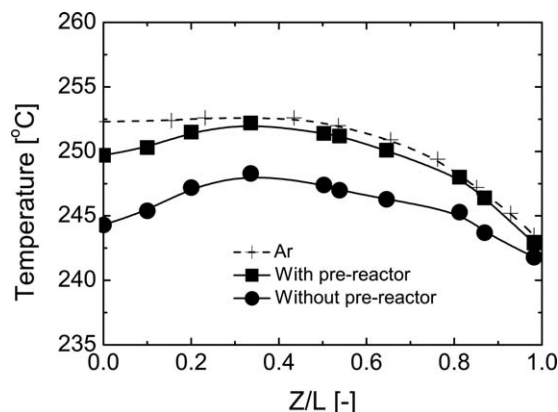


Figure 12. Temperature profile course along the axial direction for the bimodal CMR with/without a pre-reactor ($p_R = 101.3$ kPa, $p_P = 10$ kPa, $F_{\text{MCH},0} = 4 \times 10^{-6}$ mol s^{-1}).

conditions of Ar flow (without feeding reactants), probably due to insufficient insulation and/or nonhomogeneous heating. For MCH decomposition without the use of a prereactor, the temperature at the inlet of the membrane dropped by 8 to 244°C because of the endothermic reaction, then approached a temperature profile that was similar to that for Ar flow, suggesting that the MCH decomposition occurred mainly in the initial portion of the membrane. It is also worth mentioning that the temperature at the end of the membrane was still lower than that for Ar flow, indicating that the MCH decomposition was enhanced by H_2 extraction. This was confirmed by simulation when the prereactor was applied, the average temperature inside the membrane was higher than when a prereactor was not used. The temperature at the inlet was decreased 3°C compared with that during Ar flow. Higher temperature along the reactor could result in an increase in both the reaction rate and the membrane performance, which includes H_2 permeance and H_2/TOL selectivity. Thus, the increase in average temperature inside the bimodal CMR coupled with a prereactor is considered to be one theoretical explanation for the enhancement in MCH conversion in Figure 11. Moreover, as a prereactor was introduced into our H_2 production system, MCH was prereacted and MCH decomposition reached an equilibrium conversion of 0.44 at the outlet of the prereactor, which could have reduced the heat load on the bimodal CMR. Therefore, it could be concluded that the performance of the bimodal CMR for MCH decomposition was effectively enhanced by the assistance of a prereactor.

Conclusions

In the present study, a BTESE-derived organosilica membrane was fabricated and applied to a bimodal CMR for the dehydrogenation of MCH to TOL for H_2 production. Single-gas permeation characteristics for the as-prepared membrane showed a high selectivity for H_2 over TOL of 16,000, with a H_2 permeance of 10^{-6} mol $\text{m}^{-2} \text{s}^{-1} \text{Pa}^{-1}$, at 200°C. The effect of operating conditions on the performance of the CMR with respect to MCH conversion, H_2 yield, H_2 purity, H_2 flow rate, and H_2 recovery ratio was experimentally investigated for reaction temperature, MCH feed flow rate and feed pressure, H_2 extraction, MCH conversion and total H_2 flow rate all were increased due to the shift in the

reaction equilibrium. H_2 flow with a purity higher than 99.8% was obtained in the permeate stream because the as-prepared BTESE-derived membrane was almost impermeable for MCH and TOL. The H_2 recovery ratio was as high as 0.99 under an increased feed pressure that significantly improved the efficiency of the H_2 production system.

A 1-D mathematical model was developed and employed to simulate the MCH dehydrogenation in a cocurrent, isothermal, plug-flow-type membrane reactor with selective H_2 removal from the reaction side. The simulations used a fitted catalyst loading and were in good agreement with the experimental results, which verified that the proposed model was effective in predicting the performance of the bimodal CMR. However, the fitting may not be perfect for practical prediction of CMRs. We believe the development of more detailed and sophisticated simulation models, which include profiles of temperature, pressure, concentration (partial pressure) in both axial and radial directions, will be definitely important.

A system combining a fixed-bed prereactor and a CMR was proposed for MCH dehydrogenation. This system enhanced the driving force for H_2 extraction and increased the average temperature along the membrane, and thus resulted in an improvement in MCH conversion.

Notation

F = feed-side molar flow rate, mol s^{-1}
 G = purity of hydrogen, dimensionless
 J = production rate per unit reactor volume, mol $\text{m}^{-3} \text{s}^{-1}$
 k_1 = reaction rate constant, mol $\text{s}^{-1} \text{kg}_{\text{cat}}^{-1} \text{Pa}^{-1}$
 K_{eq} = equilibrium constant, Pa^3
 p = partial pressure, Pa
 p_R = feed-side pressure, Pa
 p_P = permeate-side pressure, Pa
 P = gas permeance, mol $\text{m}^{-2} \text{s}^{-1} \text{Pa}^{-1}$
 Q = permeate-side molar flow rate, mol s^{-1}
 r_d = reaction rate of MCH dehydrogenation, mol $\text{s}^{-1} \text{kg}_{\text{cat}}^{-1}$
 R = H_2 recovery ratio, dimensionless
 s = membrane area per unit membrane axial length, $\text{m}^2 \text{m}^{-1}$
 T = absolute temperature, K
 T_r = temperature inside membrane, °C
 w_{cat} = catalyst weight per unit membrane axial length, kg m^{-1}
 w_{Pt} = weight of Pt catalysts, g
 x = feed-side mole fraction, dimensionless
 X = conversion of MCH, dimensionless
 y = permeate-side mole fraction, dimensionless
 Y = yield of hydrogen, dimensionless
 z = axial coordinate, m

Subscripts

i = component i
 0 = inlet of the membrane reactor
 L = outlet of the membrane reactor

Literature Cited

- Turner JA. Sustainable hydrogen production. *Science*. 2004;305:972–974.
- Palo DR, Dagle RA, Holladay JD. Methanol steam reforming for hydrogen production. *Chem Rev*. 2007;107:3992–4021.
- Grochala W, Edwards PP. Thermal decomposition of the non-interstitial hydrides for the storage and production of hydrogen. *Chem Rev*. 2004;104:1283–1315.
- Crabtree RH. Hydrogen storage in liquid organic heterocycles. *Energy Environ Sci*. 2008;1:134–138.
- Teichmann D, Arlt W, Wasserscheid P, Freymann R. A future energy supply based on liquid organic hydrogen carriers (LOHC). *Energy Environ Sci*. 2011;4:2767–2773.
- Alhumaidan F, Cresswell D, Garforth A. Hydrogen storage in liquid organic hydride: producing hydrogen catalytically from methylcyclohexane. *Energy Fuels*. 2011;25:4217–4234.

7. Baker R. *Membrane Technology and Applications*, 2nd ed. West Sussex: Wiley, 2004.
8. Li NN, Fane AG, Ho WSW, Matsuura T. *Advanced Membrane Technology and Applications*. New Jersey: Wiley, 2008.
9. Paturzo L, Basile A, Drioli E. High temperature membrane reactors and integrated membrane operations. *Rev Chem Eng*. 2002;18:511–551.
10. Anderson M, Lin YS. Carbon dioxide separation and dry reforming of methane for synthesis of syngas by a dual-phase membrane reactor. *AIChE J*. 2013;59:2207–2218.
11. Li K. *Ceramic Membranes for Separation and Reaction*. West Sussex: Wiley, 2007.
12. Itoh N. A membrane reactor using palladium. *AIChE J*. 1987;33:1576–1578.
13. Crisculi A, Basile A, Drioli E, Loiacono O. An economic feasibility study for water gas shift membrane reactor. *J Membr Sci*. 2001;181:21–27.
14. Augustine AS, Ma YH, Kazantzis NK. High pressure palladium membrane reactor for the high temperature water–gas shift reaction. *Int J Hydrogen Energy*. 2011;36:5350–5360.
15. Tsai CY, Dixon AG, Moser WR, Ma YH. Dense perovskite membrane reactors for partial oxidation of methane to syngas. *AIChE J*. 1997;43:2741–2750.
16. Jin W, Li S, Huang P, Xu N, Shi J, Lin YS. Tubular lanthanum cobaltite perovskite-type membrane reactors for partial oxidation of methane to syngas. *J Membr Sci*. 2000;166:13–22.
17. Wei Y, Yang W, Caro J, Wang H. Dense ceramic oxygen permeable membranes and catalytic membrane reactors. *Chem Eng J*. 2013;220:185–203.
18. Coronas J, Santamaria J. State-of-the-art in zeolite membrane reactors. *Top Catal*. 2004;29:29–44.
19. McLeary EE, Jansen JC, Kapteijn F. Zeolite based films, membranes and membrane reactors: progress and prospects. *Microporous Mesoporous Mater*. 2006;90:198–220.
20. Julbe A, Farrusseng D, Guizard C. Porous ceramic membranes for catalytic reactors — overview and new ideas. *J Membr Sci*. 2001;181:3–20.
21. Jiang H, Meng L, Chen R, Jin W, Xing W, Xu N. A novel dual-membrane reactor for continuous heterogeneous oxidation catalysis. *Ind Eng Chem Res*. 2011;50:10458–10464.
22. Armor JN. Applications of catalytic inorganic membrane reactors to refinery products. *J Membr Sci*. 1998;147:217–233.
23. Tsuru T, Yamaguchi K, Yoshioka T, Asaeda M. Methane steam reforming by microporous catalytic membrane reactors. *AIChE J*. 2004;50:2794–2805.
24. Tsuru T, Morita T, Shintani H, Yoshioka T, Asaeda M. Membrane reactor performance of steam reforming of methane using hydrogen-permselective catalytic SiO₂ membranes. *J Membr Sci*. 2008;316:53–62.
25. Tsuru T. Development of metal-doped silica membranes for increased hydrothermal stability and their applications to membrane reactors for steam reforming of methane. *J Jpn Petrol Inst*. 2011;54:277–286.
26. Gallucci F, Paturzo L, Basile A. A simulation study of the steam reforming of methane in a dense tubular membrane reactor. *Int J Hydrogen Energy*. 2004;29:611–617.
27. Li G, Kanezashi M, Lee HR, Maeda M, Yoshioka T, Tsuru T. Preparation of a novel bimodal catalytic membrane reactor and its application to ammonia decomposition for CO_x-free hydrogen production. *Int J Hydrogen Energy*. 2012;37:12105–12113.
28. Li G, Kanezashi M, Yoshioka T, Tsuru T. Ammonia decomposition in catalytic membrane reactors: simulation and experimental studies. *AIChE J*. 2013;59:168–179.
29. Jeong BH, Sotowa K, Kusakabe K. Catalytic dehydrogenation of cyclohexane in an FAU-type zeolite membrane reactor. *J Membr Sci*. 2003;224:151–158.
30. Akamatsu K, Ohta Y, Sugawara T, Hattori T, Nakao S. Production of hydrogen by dehydrogenation of cyclohexane in high-pressure (1–8 atm) membrane reactors using amorphous silica membranes with controlled pore sizes. *Ind Eng Chem Res*. 2008;47:9842–9847.
31. Akamatsu K, Ohta Y, Sugawara T, Kanno N, Tonokura K. Stable high-purity hydrogen production by dehydrogenation of cyclohexane using a membrane reactor with neither carrier gas nor sweep gas. *J Membr Sci*. 2009;330:1–4.
32. Ferreira-Aparicio P, Roderiguez-Ramos I, Guerrero-Ruiz A. On the performance of porous vycor membranes for conversion enhancement in the dehydrogenation of methylcyclohexane to toluene. *J Catal*. 2002;212:182–192.
33. Oda K, Akamatsu K, Sugawara T, Kikuchi R, Segawa A, Nakao S. Dehydrogenation of methylcyclohexane to produce high-purity hydrogen using membrane reactors with amorphous silica membranes. *Ind Eng Chem Res*. 2010;49:11287–11293.
34. Amirabadi S, Kabiri S, Vakili R, Iranshahi D, Rahimpour MR. Differential evolution strategy for optimization of hydrogen production via coupling of methylcyclohexane dehydrogenation reaction and methanol synthesis process in a thermally coupled double membrane reactor. *Ind Eng Chem Res*. 2013;52:1508–1522.
35. Ali JK, Newson EJ, Rippin DWT. Exceeding equilibrium conversion with a catalytic membrane reactor for the dehydrogenation of methylcyclohexane. *Chem Eng Sci*. 1994;49:2129–2134.
36. Tsuru T, Shintani H, Yoshioka T, Asaeda M. A bimodal catalytic membrane having a hydrogen-permselective silica layer on bimodal catalytic support: preparation and application to the steam reforming of methane. *Appl Catal A Gen*. 2006;302:78–85.
37. Li G, Yada K, Kanezashi M, Yoshioka T, Tsuru T. Methylcyclohexane dehydrogenation in catalytic membrane reactors for efficient hydrogen production. *Ind Eng Chem Res*. 2013;52:13325–13332.
38. Kanezashi M, Yada K, Yoshioka T, Tsuru T. Design of silica networks for development of highly permeable hydrogen separation membranes with hydrothermal stability. *J Am Chem Soc*. 2009;131:414–415.
39. Kanezashi M, Yada K, Yoshioka T, Tsuru T. Organic–inorganic hybrid silica membranes with controlled silica network size: preparation and gas permeation characteristics. *J Membr Sci*. 2010;348:310–318.
40. Li G, Niimi T, Kanezashi M, Yoshioka T, Tsuru T. Equilibrium shift of methylcyclohexane dehydrogenation in a thermally stable organo-silica membrane reactor for high-purity hydrogen production. *Int J Hydrogen Energy*. 2013;38:15302–15306.
41. Niimi T, Nagasawa H, Kanezashi M, Yoshioka T, Ito K, Tsuru T. Preparation of BTESE-derived organosilica membranes for catalytic membrane reactors of methylcyclohexane dehydrogenation. *J Membr Sci*. 2014;455:375–383.
42. Ali JK, Baiker A. Dehydrogenation of methylcyclohexane to toluene in a pilot-scale membrane reactor. *Appl Catal A Gen*. 1997;155:41–57.
43. Usman M, Cresswell D, Garforth A. Detailed reaction kinetics for the dehydrogenation of methylcyclohexane over Pt catalyst. *Ind Eng Chem Res*. 2012;51:158–170.
44. Funke HH, Argo AM, Falconer JL, Noble RD. Separations of cyclic, branched, and linear hydrocarbon mixtures through silicalite membranes. *Ind Eng Chem Res*. 1997;36:137–143.
45. Lee HR, Kanezashi M, Shimomura Y, Yoshioka T, Tsuru T. Evaluation and fabrication of pore-size-tuned silica membranes with tetraethoxydimethyl disiloxane for gas separation. *AIChE J*. 2011;57:2755–2765.
46. Okubo T, Haruta K, Kusakabe K, Morooka S, Anzai H, Akiyama S. Equilibrium shift of dehydrogenation at short space-time with hollow fiber ceramic membrane. *Ind Eng Chem Res*. 1991;30:614–616.
47. Kniep J, Lin YS. Partial oxidation of methane and oxygen permeation in SrCoFeO_x membrane reactor with different catalysts. *Ind Eng Chem Res*. 2011;50:7941–7948.

Manuscript received Oct. 9, 2014, and revision received Jan. 15, 2015.